

Supporting Information

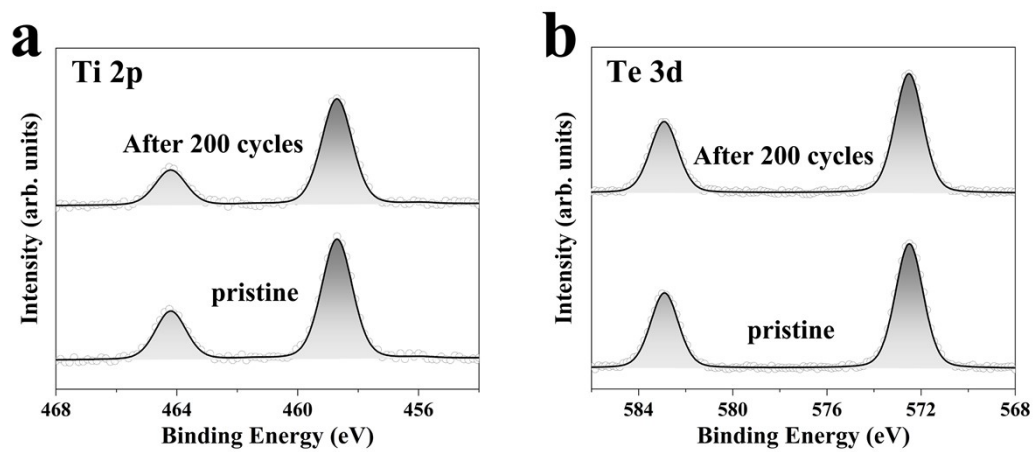


Fig. S1. The XPS spectra of (a) Ti 2*p* and (b) Te 3*d* for TiTe₂ electrode at diverse states.

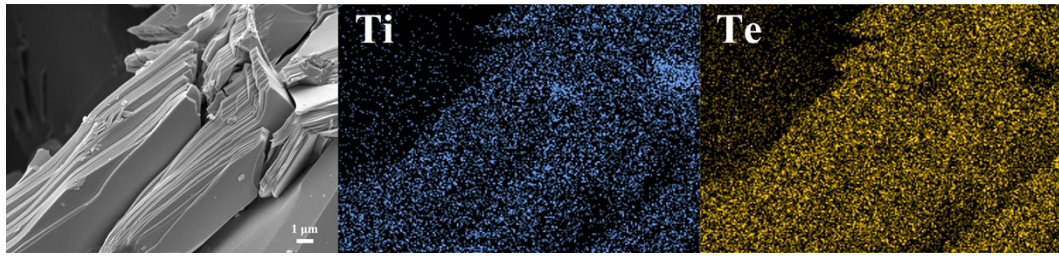


Fig. S2. The SEM image with corresponding EDS mapping for TiTe_2 .

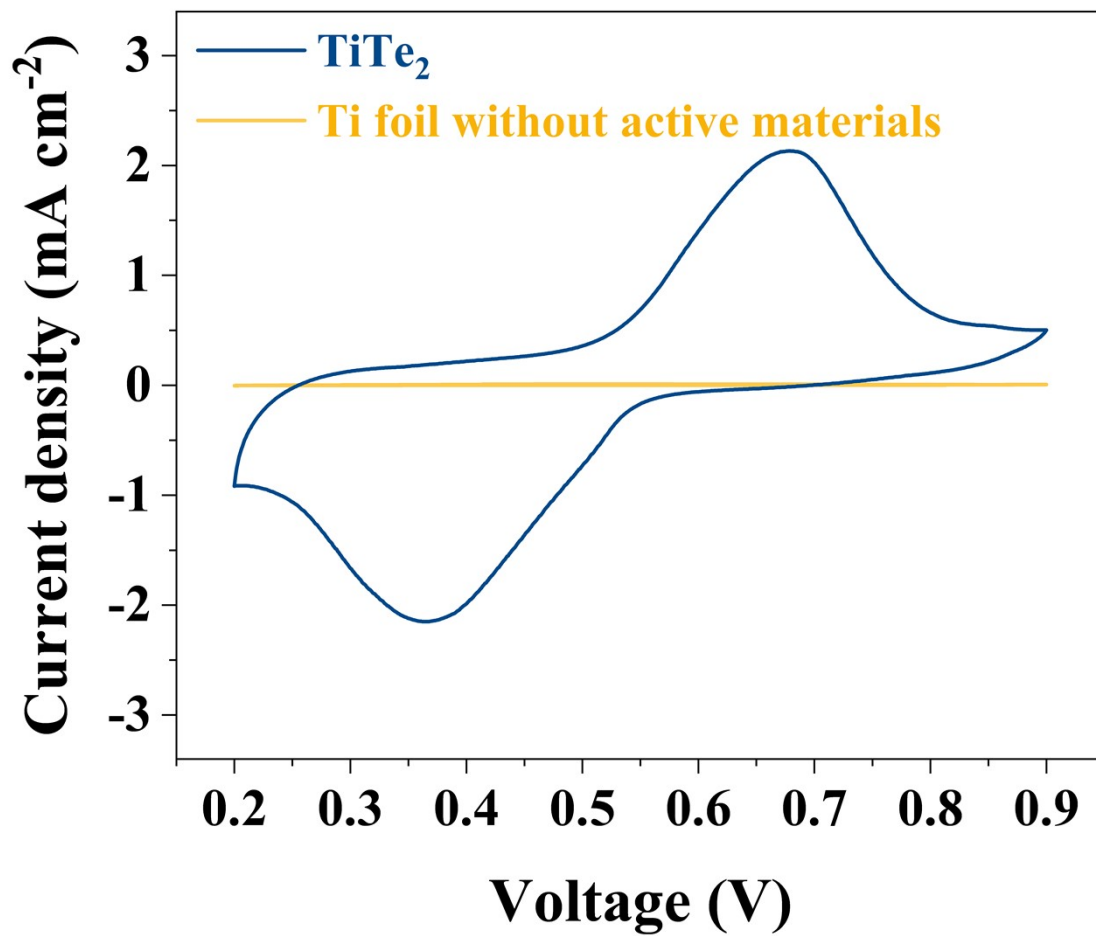


Fig. S3. The CV curves for the Ti foil electrode without active materials and TiTe₂ electrode in 3 M ZnSO₄ electrolyte at 0.6 mV s⁻¹.

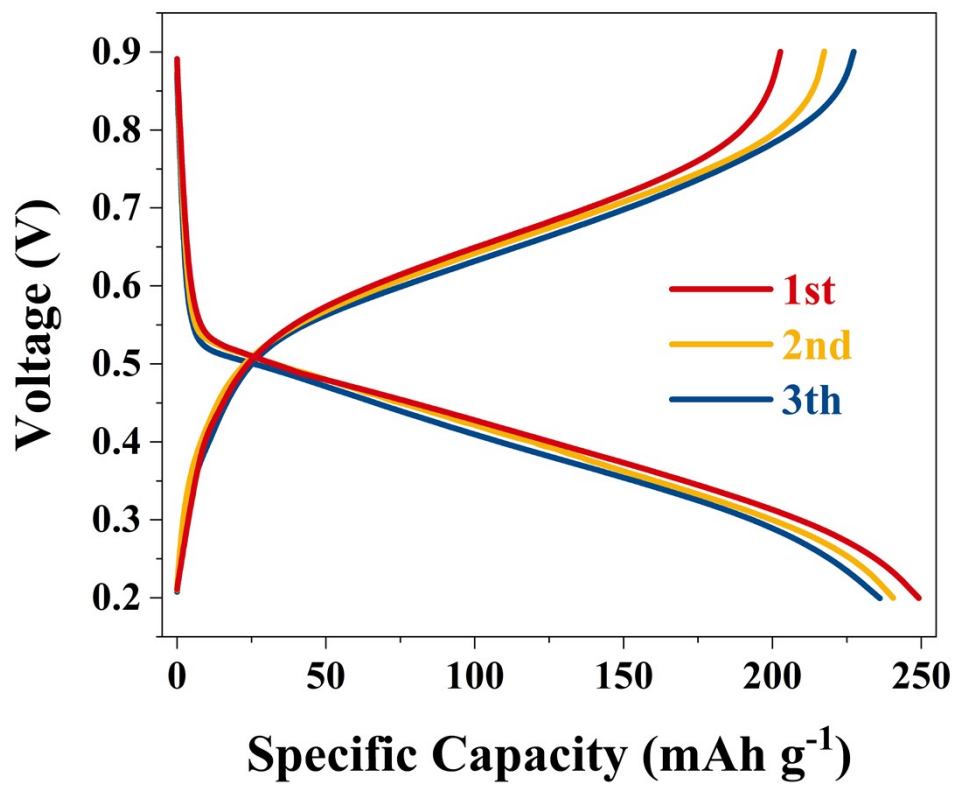


Fig. S4. The charge/discharge curves of the non-activated TiTe_2 electrode for the first three cycles at a current rate of 0.05 A g^{-1} .

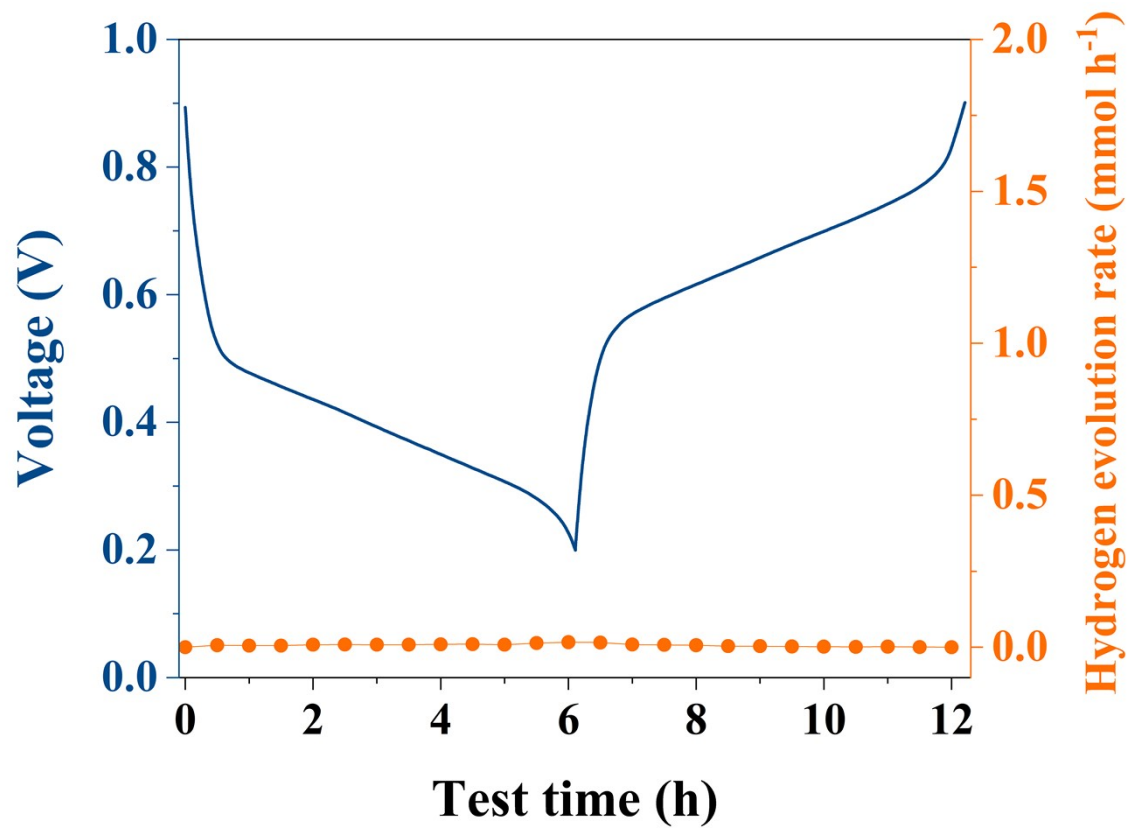


Fig. S5. The hydrogen evolution flux upon in situ DEMS test of the TiTe₂ electrode.

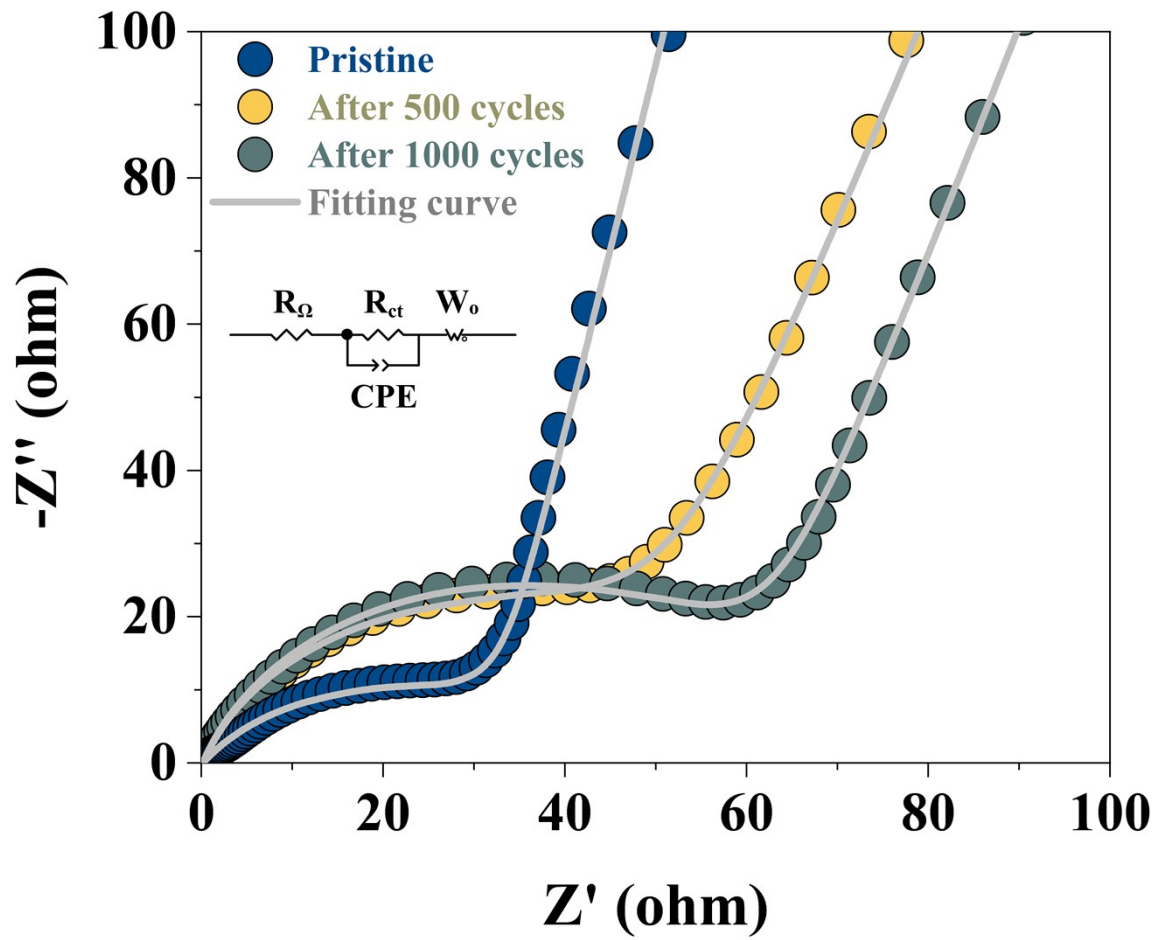


Fig. S6. Nyquist plots with the corresponding equivalent circuit for TiTe_2 electrode at the pristine state, after 500 cycles, and after 1000 cycles.

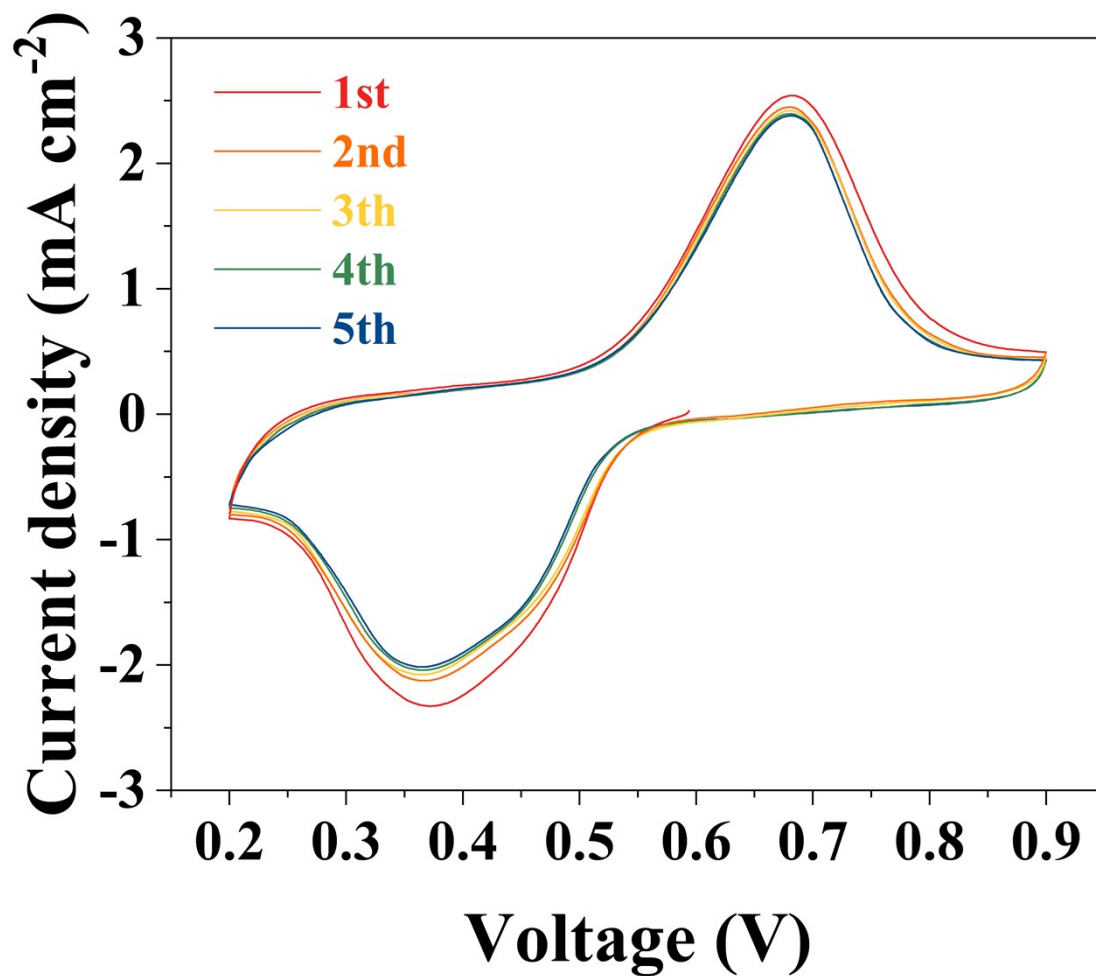


Fig. S7. The CV curves of the non-activated TiTe_2 electrode for the first five cycles at 0.6 mV s^{-1} .

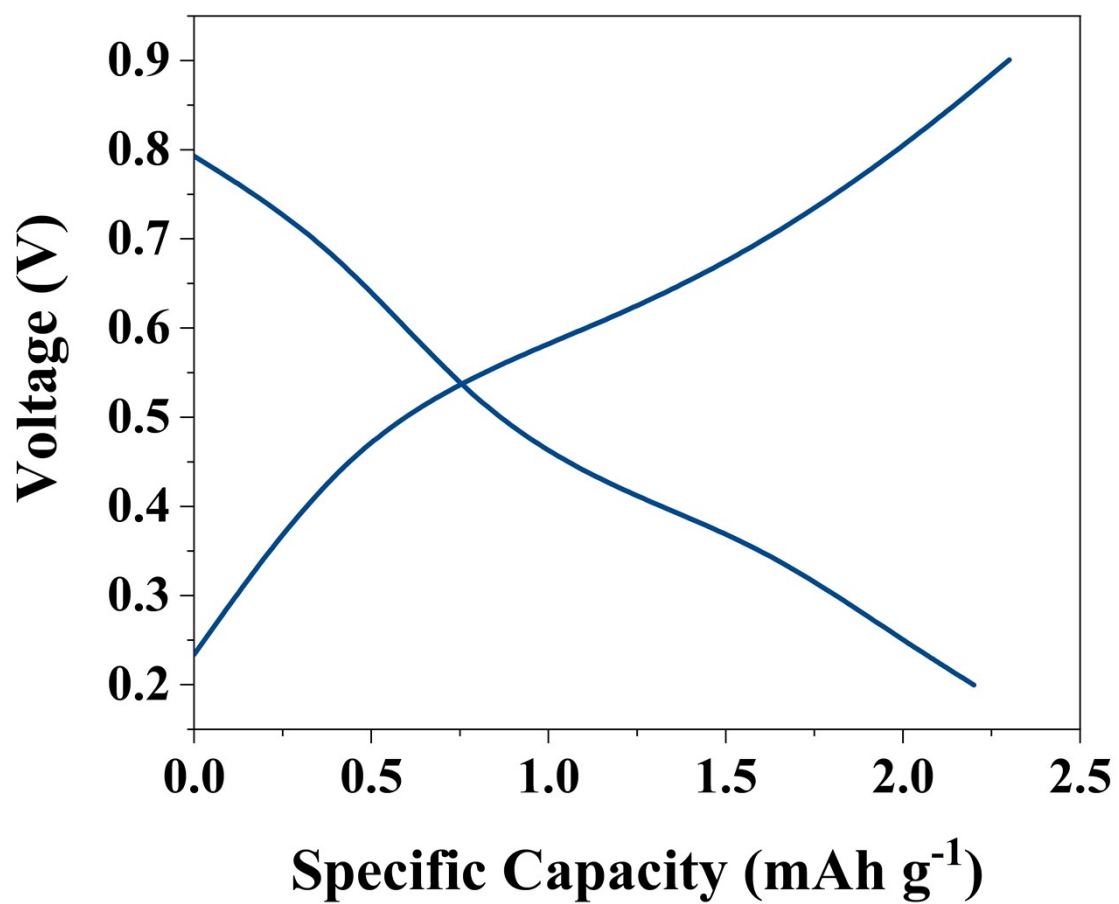


Fig. S8. The charge and discharge curves for the TiTe₂ electrode in the 3 M H₂SO₄ electrolyte.

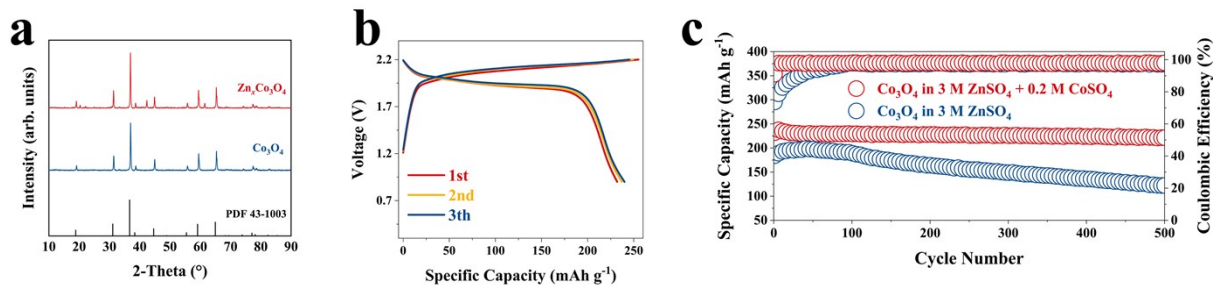


Fig. S9. (a) The XRD patterns of $Zn_xCo_3O_4$ and Co_3O_4 . (b) The charge/discharge curves for the $Zn_xCo_3O_4$ electrode in the 3 M $ZnSO_4$ + 0.2 M $CoSO_4$ electrolyte. (c) The cycling performances for $Zn_xCo_3O_4$ electrodes in the 3 M $ZnSO_4$ + 0.2 M $CoSO_4$ and 3 M $ZnSO_4$ electrolyte at $0.1\ A\ g^{-1}$.

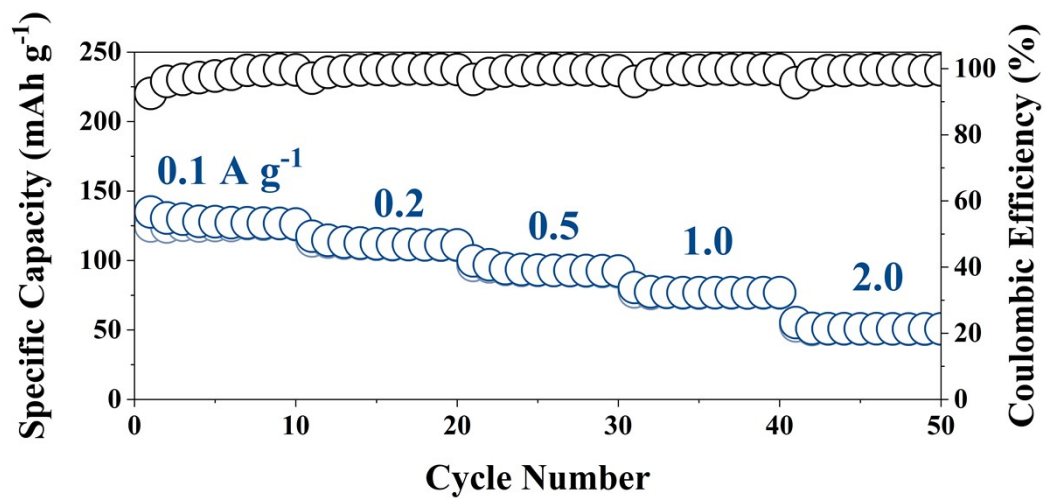


Fig. S10. The rate capability of the $TiTe_2||Zn_xCo_3O_4$ pouch cell from 0.1 to 2.0 $A\ g^{-1}$.